

A Case Study on Biological Activity in a Surface-Bound Multicomponent System: The Biotin–Streptavidin–Peroxidase System[†]

Rolf Chelkowski, Andreas Prekelt, Christian Grunwald,* and Christof Wöll

Physikalische Chemie I, Ruhr-Universität Bochum, 44780 Bochum, Germany

Received: June 21, 2007; In Final Form: August 24, 2007

The adsorption of multiple protein layers on biotinylated organic surfaces has been characterized using surface plasmon resonance (SPR) and atomic force microscopy (AFM). Diffusion-limited loading of the biotinylated self-assembled monolayers (SAMs) ensures a precise control of the streptavidin surface density. For the subsequent interaction with biotinylated peroxidase, SPR data hint at a streptavidin density dependent orientation during peroxidase adsorption. Microcontact printed well-defined two-dimensional patterned surfaces of biotinylated organothiols and protein-resistant OEG-thiols allow an in-situ differentiation of specific and nonspecific adsorption (e.g., mono- vs multilayer adsorption). Additionally, the very important issue of biological activity of surface-bound enzymes is addressed by comparing the enzyme activities in solution with that for surface-bound species.

Introduction

The exceptional tight binding of biotin to biotin-binding proteins (e.g., avidin, streptavidin, or anti-biotin antibodies) was previously used for the creation of supermolecular structures.^{1,2} Covalent or noncovalent coupling of biomolecules, e.g., DNA^{3–6} or proteins^{7,8} and especially enzymes,^{2,9} to streptavidin has been reported by different groups and is today a routine process in analytical sandwich assays.^{10–12} In these assays streptavidin serves as a biological glue interfacing analyte (e.g., biotinylated DNA) and a signal amplification reporting system (e.g., biotinylated peroxidase). The sandwich functionality is strongly facilitated by the avidine's tetrameric cubelike structure presenting in total four biotin-binding pockets with two of each placed on opposite faces of the cube. It should be mentioned that even today most sandwich assays work in volume (e.g., microwell plates) and are not surface based. However, starting from biotinylated surfaces allows for a subsequent attachment of further biotinylated moieties and thus provides an elegant way to build multicomponent systems in a step-by-step fashion.¹ All biotin-streptavidin architectures take advantage of the high selectivity and affinity ($K_A = 10^{15} \text{ M}^{-1}$) of biotin to its binding pocket.²

When creating multicomponent and multilayer architectures from scratch on mixed biotinylated self-assembled monolayers, one has to consider that despite the tight biotin–streptavidin interaction some unspecific interaction of the biomolecules to each other or to the non-biotinylated matrix can occur. Controlling unspecific adsorption of proteins to surfaces is an important medical (e.g., coating of medical implants^{13,14}) and biotechnological (e.g., cultivation of cells¹⁵) issue. As a result, the development of new surface coatings resistant to unspecific adsorption is a topic that currently attracts a large amount of interest.

Unspecific adsorption is a somewhat mystical subject, and clearly there is a disturbing lack of information about the

microscopic origins of this phenomenon. For many specifically interacting species (e.g., biotin and its binding pocket in the avidines), crystal structures are available, highlighting the very well-defined molecular arrangements of the interacting biomolecules. In contrast, the unspecific interactions between proteins and surfaces are by definition nonspecific and therefore not well defined. In fact, for unspecifically adsorbed proteins the molecular arrangement is not defined precisely but corresponds to a complex ensemble of different arrangements, each comprising multiple and different weak protein surface interactions. The different individual arrangements are difficult to access.

Most often, the total amount of unspecific adsorbed proteins is quantified, e.g., using SPR,¹⁶ AFM,^{17,18} or fluorescence.¹⁹ An important question is whether also unspecifically bound proteins retain their biological function. Whereas in most cases unspecific adsorption is accompanied by an unfolding of the protein (resulting in a loss of biological function), generally the activity of the adsorbed proteins also needs to be determined.

In this study peroxidase was chosen as model enzyme because the structure and enzymatic mechanism²⁰ are well-known. Furthermore, peroxidase is widely used as a reporting enzyme in many applications (e.g., ELISA assays) and thus all needed compounds are commercially available (e.g., Sigma P9568 and T8665). Briefly summarizing, the determination of enzymatic activity is based on the conversion of the colorless chromogen 3,3',5,5'-tetramethylbenzidine (TMB) into a blue product (TMB charge-transfer complex). By addition of an acidic stopping solution (H_2SO_4) the enzymatic reaction is terminated and the charge-transfer complex is converted to a stable yellow dye that can be read at 450 nm.

Microcontact printing (μCP), as introduced by Whitesides et al.,²¹ is a convenient and low-cost method for producing lateral patterned surfaces offering the opportunity to perform high-quality differential measurements using one and the same sample.¹⁹ Atomic force and fluorescence microscopy as well as surface plasmon resonance are well-known methods to investigate interactions of proteins with self-assembled well-engineered organic thin film interfaces. Offering the opportunity to characterize the adsorption of biomolecules in situ under

[†] Part of the "Giacinto Scoles Festschrift".

* To whom correspondence should be addressed. E-mail: Christian.Grunwald@gmx.net. Phone: +49-(0)234-32-25529. Fax: +49-(0)234-32-14182.

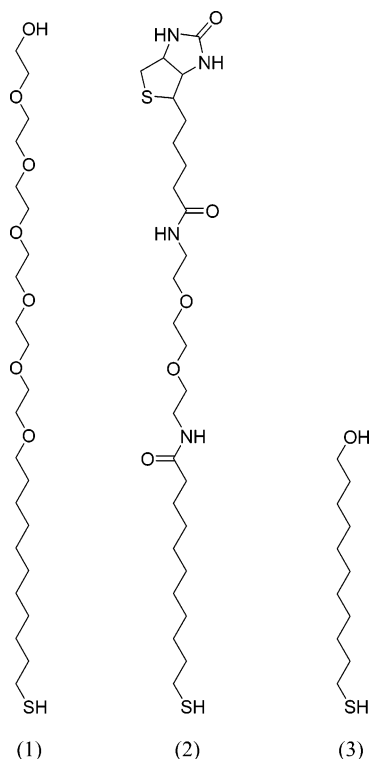


Figure 1. Organothiols that have been used throughout this study: (1) protein resistant oligo(ethylene glycol)-thiol (OEG-thiol); (2) biotinylated thiol (biotin-thiol); (3) mercapto-undecanol (OH-thiol).

physiological conditions (e.g., in buffers) in real-time, these techniques soon became widely accepted in biomolecular surface science.

Materials and Methods

Substrate Preparation for SPR. D263 thin glass (Schott) with dimensions of 10 mm \times 10 mm \times 0.3 mm were rinsed with absolute ethanol (Riedel-de Haën), dried in a stream of nitrogen, and then installed in a Leybold Inficon XTC/2 metal evaporator. First a 12 Å layer of titanium was deposited at 1 Å s^{-1} to improve the adhesion of the subsequently deposited gold layer. Gold was evaporated at a rate of 15 Å s^{-1} , the final thickness amounts to approximately 485 Å. Evaporation was done at room temperature and a pressure of approximately 10^{-7} mbar. After metal deposition, the gold-covered glass slides were incubated for 2 days in ethanolic solutions containing a mixture of OH- and biotin-terminated thiols (OH- and biotin-thiol; see Figure 1 for the structures). The final thiol concentration was kept constant at 1 mM while varying the relative content of the biotin-thiol between 0 and 100 mol %. Subsequently, the SAM surfaces were rinsed with ethanol before attaching the slides to plastic chips (Biacore) using a double-sided polyester tape (tape 415, 3M). In the same way different organic surfaces have been prepared (e.g., hydrophobic surfaces using octadecanethiols). A commercial surface plasmon resonance system (Biacore 3000) was used to record the real-time kinetics of the protein adsorption to the different organic surfaces.

Substrate Preparation for AFM. The preparation process is similar to the deposition process described for the SPR substrates (see above). Instead of glass, polished silicon wafers with a (100) surface termination were used (Prolog Semicor Ltd.). Prior to the metal deposition they were rinsed with absolute acetone (Fluka) and ethanol (Riedel-de Haën). Titanium was deposited to a thickness of 80 Å at a rate of 2 Å s^{-1} ; subsequently, a 1200 Å layer of gold was added using a rate of

15 Å s^{-1} . The gold covered silicon wafers were cut into pieces of 10 mm \times 10 mm and further functionalized using micro contact-printing.

Microcontact Printing (μ CP). Lateral patterned SAMs were fabricated using a procedure previously described.²² Briefly, liquid poly(dimethylsiloxane) (PDMS; Sylgard 184, Dow Corning) is poured over a master object (e.g., patterned silicon wafer or glass) and cured by polymerization. Elastic stamps are obtained by peeling the PDMS replicate off the master object. Because the master object can be reused many times, numerous stamps can be produced from one master object. During these studies a silicon wafer was used as the master object to yield a periodic stamp surface consisting of squares (3 μ m \times 3 μ m). Each square is separated in x - and y -directions by 3 μ m from the next square.

Before stamping, the PDMS replicate was loaded with 1 mM ethanolic solutions of a protein resistant thiol (OEG-thiol; see Figure 1 for the structure). Therefore the patterned stamp surface was incubated for 60 s with an 80 μ L droplet of the ethanolic thiol solution. Then the stamp was dried in a stream of nitrogen and gently pressed toward the gold surface for 90 s. Finally, the stamp was removed and the samples were first cleaned with ethanol and dried under a stream of nitrogen and then immersed for 90 s in an ethanolic solution containing a mixture of OH- and biotin-terminated thiols (OH- and biotin-thiol; see Figure 1 for the structures). The total thiol concentration of the mixtures was kept constant at \sim 1 mM. After immersion the laterally structured self-assembled monolayers (SAMs) were once again rinsed with absolute ethanol and dried under a stream of nitrogen.

Substrate Preparation for Activity Tests. Substrate preparation was similar to that described for the SPR samples (see above). Instead of thin glass, conventional microscopy slides (BK7, Menzel, 76 mm \times 26 mm \times 1 mm) were used as the supporting material. After metal deposition the slides were cut into pieces of 2 mm \times 10 mm and incubated in ethanolic thiol solutions as described for the SPR substrate preparation (see above). After SAM formation the samples were washed intensively with copious amounts of ethanol and blown dry in a stream of nitrogen.

SPR Measurements. A commercial surface plasmon resonance system (Biacore 3000) was used to record the real-time kinetics of protein adsorption. At first the main attention was turned to find suitable incubation conditions for streptavidin and the biotinylated peroxidase protein. Therefore a first set of experiments was aimed at controlling the amount of streptavidin adsorbing to the organic thin film surface. During SAM preparation the biotin-thiol concentrations were varied systematically to yield organic surfaces with different biotin content. Then these surfaces were loaded with streptavidin using 200 nM streptavidin solution and a contact time of 900 s. This approach seems to be straightforward but is hampered by some undesirable side effects (see Results section below). Thus, as an alternative way to control streptavidin surface adsorption, we examined diffusion-limited loading of biotinylated SAM surfaces. In this approach the biotin surface content was kept constant and streptavidin concentrations (25 and 50 nM) as well as streptavidin contact times were varied to obtain an arbitrary predetermined streptavidin surface density. Then for the positive binding control (specific streptavidin–peroxidase interaction) the biotinylated peroxidase was applied directly to streptavidin-incubated surfaces; for negative control (unspecific adsorption of peroxidase) D-biotin was added to the streptavidin-incubated surfaces before applying the biotinylated peroxidase. Addition-

ally, the unspecific adsorption of streptavidin and peroxidase to a purely OH-terminated SAM was examined. Throughout the SPR experiments a potassium phosphate buffer of the following composition was used: 0.1 M K_2HPO_4 (Sigma), 0.1 M KH_2PO_4 (Sigma), 300 mM NaCl (Baker). The pH was adjusted to 6.0 with NaOH and HCl. Only high-purity water from a MilliQ-system was used for buffer preparation. Additionally, the buffer was filtered through a sterile filter (pore size 0.2 μm) and degassed before usage. All SPR experiments were done at 25 °C. The streptavidin used in this study is a fluorescently labeled variant (Alexa-Fluor-488, Molecular Probes). A biotinylated variant of peroxidase (biotinaminocaproyl-horseradish peroxidase, Sigma Aldrich, P-9568) was used in the experiments reported here.

AFM Measurements. The AFM images were recorded using a Multimode Nanoscope IIIa (Digital Instruments). The microscope was operated in tapping mode under liquid with silicon nitride cantilevers (type NP-STT, VEECO Corp.). The force constants of these cantilevers were between 0.06 and 0.58 Nm^{-1} . The AFM was used with a 5.575 μm z -range and 150 μm x - and y -range scanner (type J Digital Instruments). Topographic images were recorded in constant force mode of the microscope. Lateral structured SAM surfaces were incubated with the protein solutions as described for the SPR measurements (see above). After incubation the samples were rinsed with high-purity MilliQ water and installed in the AFM stage with a drop (2–3 mL) of MilliQ water added on the top of the sample. Afterward the fluid cell was mounted and the tip approached to the surface of the sample.

Photometric Activity Tests. For the activity test only the maximum protein coverage was investigated because the diffusion-limited loading of the surfaces outside the biacore system by using a micropipet was not reproducible enough. SAM-coated substrates prepared for photometric activity tests were incubated for 5 min with a 200 nM streptavidin solution. Subsequently, the surface was rinsed with buffer to remove unbound protein. Then the surface was dipped for 5 min into a 100 nM solution of the biotinylated peroxidase. Again the surface was rinsed with buffer to remove loosely adsorbed proteins. After adsorption of the proteins the substrates were incubated for 5–15 min at room temperature in 1 mL of freshly prepared TMB–substrate–solution (all compounds were obtained from Sigma-Aldrich: 0.3 mM 3,3',5,5'-tetramethylbenzidine (TMB), 8 μM penicillin G, 2.15 mM phosphoric acid, 38 mM sodium dihydrogen phosphate, 1.1 mM sodium hydrogen phosphate, 0.75 mM carbamide peroxide; dissolved in a v/v mixture of 5% DMSO and 95% MilliQ water). Finally, 1 mL of 0.1 M sulfuric acid was added to stop the enzymatic reaction. Five minutes after adding the sulfuric acid solution, absorption spectra ranging from 350 to 550 nm were recorded using an UV-kon/Eppendorf spectrometer (SPECORD 200, Analytik Jena).

Results

SPR Measurements, Variation of Biotin-Thiol Concentration. The first set of experiments aimed at controlling the amount of streptavidin adsorbing to the SAM surface by adjusting the biotin-thiol concentration during SAM formation. Figure 2 summarizes the outcome of these experiments. Optimum streptavidin–biotin interaction is found for SAM prepared from ethanolic solution containing 5% biotin-thiol and 95% OH-thiol. Increasing biotin-thiol concentrations during self-assembly of the organic monolayer decreases the amount of adsorbed streptavidin. This effect has been reported in the literature before

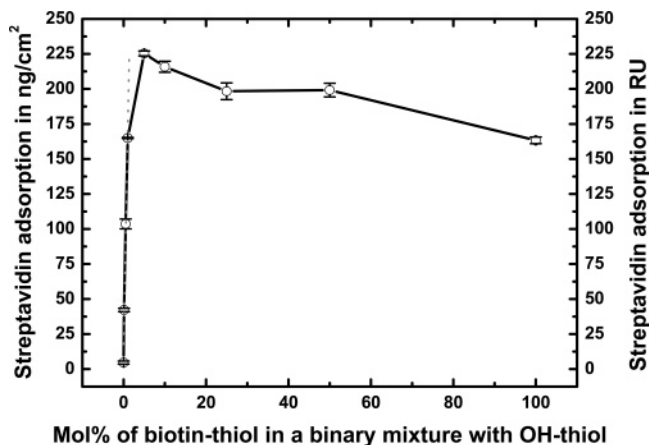


Figure 2. Adsorption of streptavidin to differently biotinylated SAMs after 900 s incubation time using 200 nM streptavidin solutions. Error bars indicate the average of four measurements each. The biotin content refers to the composition of the binary incubation mixture during SAM formation.

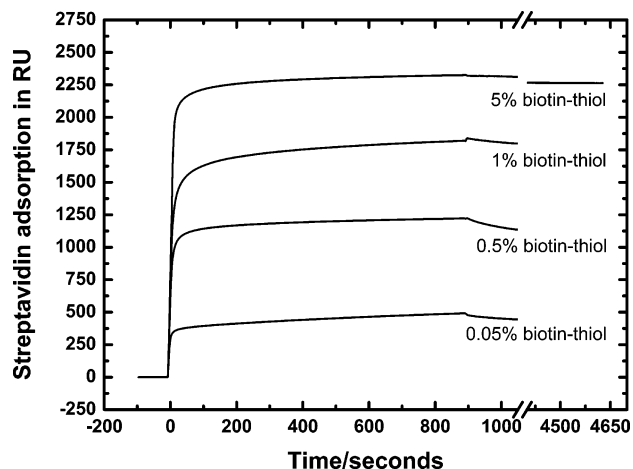


Figure 3. Real-time streptavidin adsorption kinetics for streptavidin (200 nM) adsorbing to differently biotinylated SAMs. The biotin content refers to the composition of the binary incubation mixture during SAM formation.

and is attributed to sterical interference.²³ A suboptimum binding is also observed when the biotin-thiol concentrations are kept lower than 5 mol % during self-assembly of the organic monolayer. In this concentration regime the reason for the decrease in streptavidin adsorption is due to depletion of biotin head group in the organic monolayer.

Finally, it was found that the unspecific adsorption at low mole percents of biotin-thiol is strongly dependent on the incubation conditions. One aspect is general experimental handling (e.g., impurities in solvent and vessels, dust particles) and another aspect is incubation time for the SAM formation. At low incubation times a lot of disorder is found in the SAM, promoting a significant higher unspecific adsorption in comparison to long incubated SAM surfaces (5 min, 24.9 ± 0.8 ng/cm^2 ; 2 days, 4.6 ± 1.1 ng/cm^2).

Real-time streptavidin adsorption kinetics (see Figure 3) corresponding to the experiments visualized in Figure 2 demonstrates that the streptavidin binding is a two-phase process. For clarity reasons only a selection of kinetics is shown. In the early adsorption phase streptavidin binding is linear in time; then the binding slows down more and more until the saturation level is reached. Streptavidin incubated surfaces were rinsed in long time experiments with buffer for more than 1 h with only a slight loss of streptavidin molecules (typically

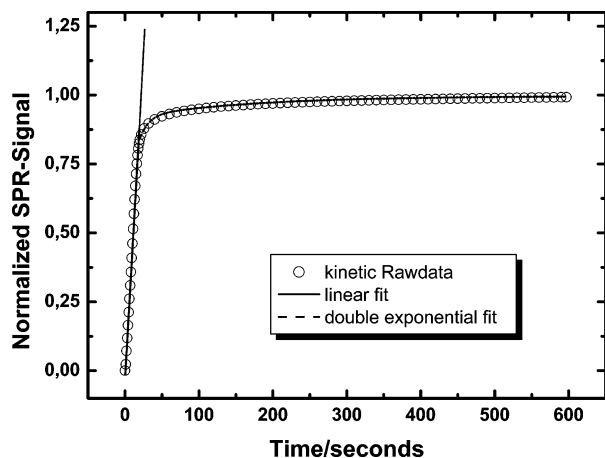


Figure 4. Detailed analysis of the two phase streptavidin adsorption kinetics (5% biotin-thiol, 200 nM streptavidin). Prior to fitting, the kinetic amplitude has been normalized. The initial linear phase comprises 80% of the kinetic amplitude, and the remaining 20% show a double exponential behavior. For detailed discussion see the text.

TABLE 1: Comparison of Single- and Double-Exponential Fits to the Second Nonlinear Adsorption Phase during Streptavidin Binding toward a Biotinylated SAM (5% Biotin-Thiol)^a

monoexponential fit, $R^2 = 0.873$	$y = a(1 - \exp(-bx))$
a	0.9350 ± 0.0028
b/s^{-1}	0.0212 ± 0.00004
double-exponential fit, $R^2 = 0.997$	$y = a(1 - \exp(-bx)) + c(1 - \exp(-dx))$
a	0.5397 ± 0.0031
b/s^{-1}	0.0814 ± 0.0011
c	0.4613 ± 0.0025
d/s^{-1}	0.0062 ± 0.0001

^a Prior to fitting, the amplitude of the second phase was normalized to 1 therefore amplitudes are dimensionless.

around 2.5%). A more detailed kinetic analysis is depicted in Figure 4. Clearly the two distinct kinetic phases have been separated one from another. The linear phase hints at diffusion-limited streptavidin binding. Streptavidin binding is fast in comparison to diffusion causing a depletion layer close to the SAM surface and thus the mass transfer limits the adsorption kinetics. In the final nonlinear phase a suitable fit to kinetic raw data could only be obtained when double exponential functions were used. In Table 1 the fitting results are summarized. Please note that the adsorption signal was normalized prior to fitting. First a line was fitted to the early adsorption phase to separate linear from nonlinear adsorption behavior. The point where the kinetic raw data deviates from the linear fit was used as starting point for the nonlinear phase. The nonlinear phase was once more normalized before fitting with a double exponential model.

SPR Measurements, Diffusion-Limited Streptavidin Loading. In Figure 5 diffusion-limited streptavidin adsorption kinetics are presented. Low streptavidin surface densities ranging from 325 to 1273 RU are obtained by using a freshly prepared 25 nM streptavidin solution and varying contact times from 34 to 109 s (dashed traces, streptavidin 25 nM). A freshly prepared 50 nM streptavidin solution is used to prepare higher streptavidin surface densities amounting to 1448–2072 RU (solid traces, streptavidin 50 nM). Here, the contact time varied from 102 to 170 s. For comparison, the most upper curve (dash-dot-dash trace, streptavidin 200 nM) shows the previously discussed adsorption kinetics yielding maximum streptavidin adsorption. When inspecting the traces recorded for low and high strepta-

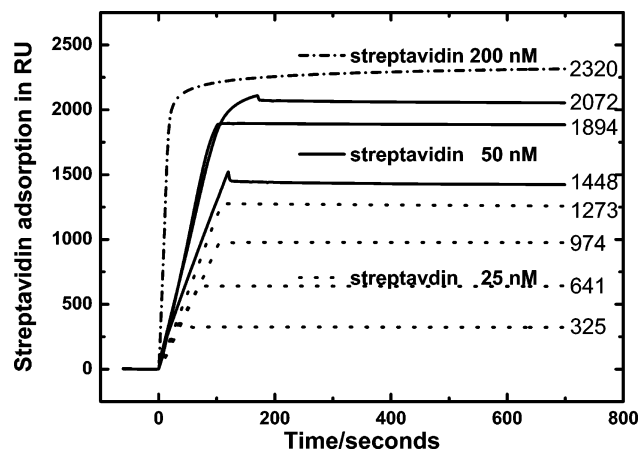


Figure 5. Diffusion-limited loading of streptavidin toward biotinylated SAMs enabling precise control of immobilization density. The biotin content was kept constant at 5% biotin-thiol during SAM formation. Streptavidin solutions are freshly diluted to the concentrations indicated.

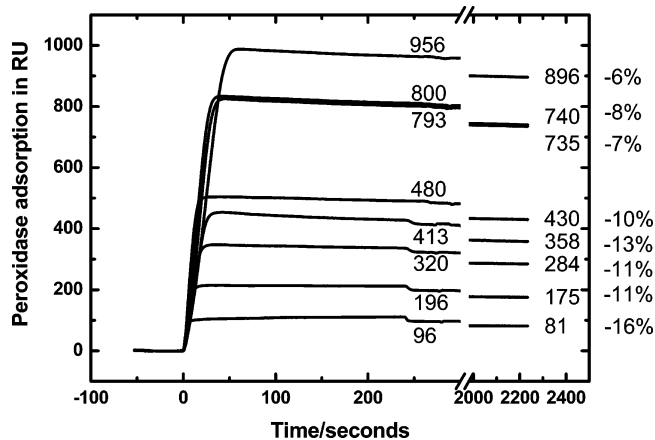


Figure 6. Subsequent adsorption of biotinylated peroxidase (100nM) toward different pre-immobilized amounts of streptavidin (see Figure 5). With increasing streptavidin surface density, more peroxidase is bound to the surface. Upon rinsing, a slight amount of protein is lost.

vidin densities, one can observe slight deviations in the slope during streptavidin loading, which is due to instabilities of the low concentrated streptavidin solution. Although freshly prepared streptavidin solutions were used on the time scale of these experiments (approximately 1–2 h), proteins adsorb from the low concentrated solution to the walls of the vessel, which is used for storing the diluted solution. Evaporation of solvent should have a counteracting effect. In this study we observed that the decrease of protein concentration dominates over the concentrating evaporation effect. Moreover, a deviation from the linear adsorption behavior is also seen in the two experiments with the highest diffusion-limited streptavidin loading (1894 and 2072 RU) at the end of the streptavidin injection. In both cases the adsorption speed is decreased because the free biotin binding sites are more and more depleted. In this phase the unsuccessful collisions between streptavidin and the SAM surface increase whereas during the linear phase each streptavidin that hits the surface will stick to the surface.

SPR Measurements, Peroxidase Adsorption. Kinetics for peroxidase adsorbing to surfaces with different levels of streptavidin surface densities are shown in Figure 6. Peroxidase adsorption from a 100 nM solution to the surface-immobilized streptavidin is fast and diffusion limited, as indicated by the linear slopes in the early adsorption phases. A saturation limit is reached within 9–56 s after injecting the peroxidase solution. However, a desorption process is superimposed on the adsorp-

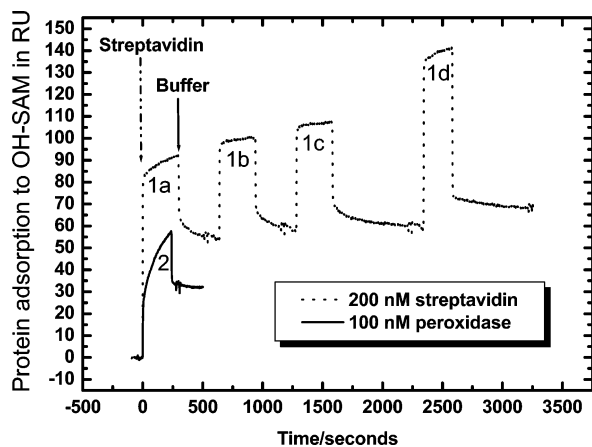


Figure 7. (Upper curve) unspecific adsorption of streptavidin toward pure OH-terminated SAM for three successive times (1a–1c) and binding of peroxidase toward this unspecific pre-adsorbed streptavidin (1d). (Lower curve) unspecific adsorption of peroxidase (2) toward pure OH-thiolate SAM. The total protein incubation time was matched to the specific binding experiments.

tion. After reaching the saturation level, especially for the peroxidase interacting with high streptavidin surface densities, a significant amount of desorption is observed. It should be noticed that desorption continues but decreases upon rinsing for more than 30 min. As will be revealed later (see Figure 9, Results and Discussion), at high streptavidin surface densities more peroxidase adsorbs (almost a one-to-one interaction) and at lower streptavidin densities a comparable weaker adsorption is seen.

SPR Measurements, Unspecific Adsorption of Streptavidin and Peroxidase. Unspecific adsorption of streptavidin and peroxidase were checked individually using OH-terminated SAM surfaces as well as D-biotin blocked streptavidin at various surface densities. Figure 7 depicts two experiments on the interaction of the proteins to OH-terminated SAMs. The dashed curve shows the unspecific adsorption of streptavidin to the OH-SAM surface. In this experiment 200 nM streptavidin solutions have been brought into contact with the surface by three subsequent 5 min injections. Multiple injections have been chosen to enable us to report on the time course of unspecific streptavidin adsorption. The total contact time is consistent with the longest incubation time used for streptavidin loading (see above and Figure 4), yielding a reasonable estimation for unspecific adsorption. Finally, a 4 min 100 nM peroxidase injection was applied to the surface to probe biotin-binding pockets. The peroxidase protein was applied to the surface at a concentration of 100 nM for 4 min, yielding a weaker unspecific adsorption in comparison to streptavidin. With reference to specific binding (streptavidin, Figures 2, 3, and 5; peroxidase, Figure 6) the observed unspecific adsorption of both proteins is weak. Further tests were undertaken because unspecific binding to the OH-terminated parts of the SAM could be modulated in the presence of different amounts of immobilized streptavidin and moreover also unspecific binding of peroxidase to streptavidin has to be considered. To clarify these issues, the experiments depicted in Figure 8 were accomplished. The bar plot shows different amounts of streptavidin that were loaded under diffusion limitation to a mixed biotin-OH-thiolate SAM. Then the immobilized streptavidin was blocked by applying 2 times a 1 mM D-biotin solution for 1 min. Subsequently, the D-biotin blocked streptavidin surfaces were incubated for 4 min with a 100 nM solution of peroxidase (inset in Figure 8). Upon application of D-biotin a slight desorption is recognized (-34 ± 31 RU), during incubation with peroxidase

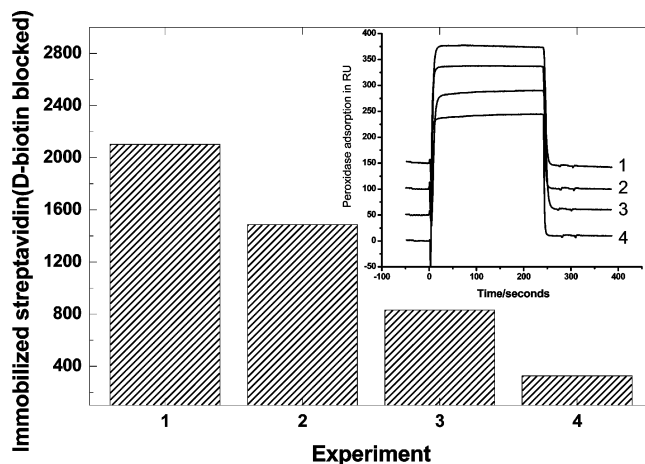


Figure 8. Biotinylated SAMs (5% biotin-thiol) loaded under the diffusion limit to four different streptavidin surface densities (bar diagram). Subsequently, all remaining biotin-binding pockets were blocked by applying a D-biotin solution (not shown). Finally, almost no unspecific adsorption is seen when a 100 nM peroxidase solution is applied to blocked streptavidin surfaces (inset line diagram).

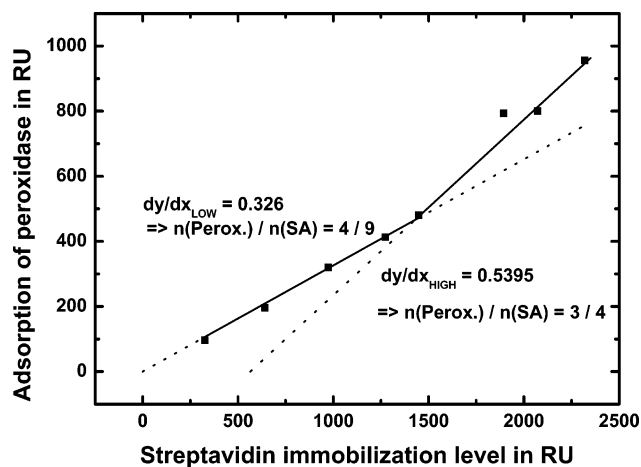


Figure 9. Specific peroxidase-to-streptavidin adsorption plotted against streptavidin surface density. From low to high streptavidin surface densities, the molecular interaction ratio changes, hinting at a reorientation of the peroxidase during adsorption toward high streptavidin surface densities. Peroxidase is an asymmetric molecule extended in one dimension.

only a very weak adsorption is found (5 ± 8 RU). During the treatment of bound streptavidin with solution of biotin no desorption of streptavidin was observed.

SPR Measurements, Correlation between Streptavidin and Peroxidase Adsorption. Finally, the molecular ratio between streptavidin and biotinylated horseradish peroxidase could be calculated using the saturation levels of the kinetics. In Figure 9 the peroxidase adsorption is plotted against the streptavidin adsorption. The lowest five pairs of peroxidase and streptavidin adsorption fit very well to a line through the origin with a slope of 0.326. From the slope an average ratio of the interacting peroxidase and streptavidin masses can be calculated. Considering the protein's molar masses (streptavidin 60 kDa and peroxidase 44 kDa) the mass ratio can be transferred into an average number of interacting molecules. For the lower part of the plot we conclude that about four peroxidase molecules are interacting with nine streptavidin molecules (1–2.25). For the higher peroxidase–streptavidin adsorption pairs a deviation from this line is observed and these pairs can be fitted to a separate line equation with a steeper slope (0.540). From this slope on average three peroxidase molecules are interacting with

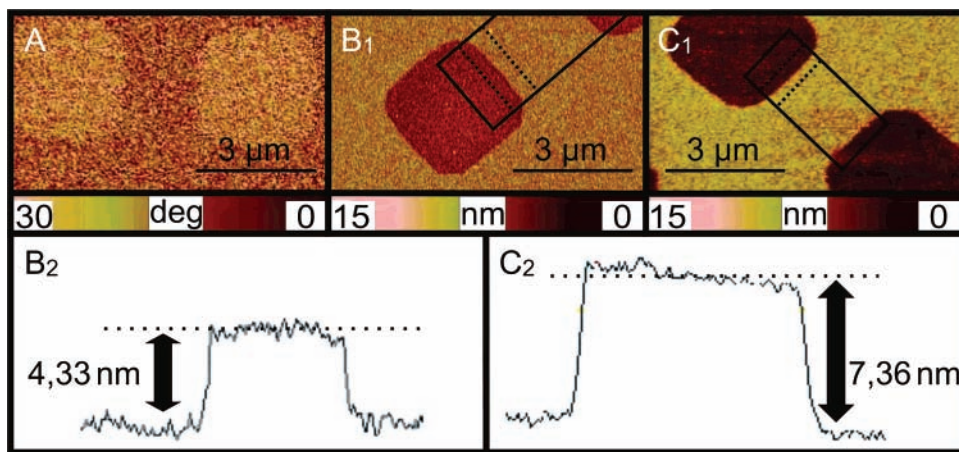


Figure 10. (A) Phase image of the surface after incubation with the OEG(6)-thiol (bright squares) and the 10% biotin-thiol (dark bridges). (B₁) Topographic height image after incubation with SA. (C₁) Topographic height image after adsorption of bHRP on the SA layer. The height contrast is increasing coherent per step of protein adsorption, as shown in section B₂ for SA and C₂ for bHRP adsorption. Section analysis shows also that no compression of the protein layer during the AFM measurement can be obtained.

four streptavidin molecules. The adsorption pair (1894 RU streptavidin; 793 RU peroxidase) is completely off the line and does not fit into any of the trends.

AFM Measurements. In Figure 10 the results for patterned SAM surfaces obtained by tapping-mode AFM are presented. The first picture (Figure 10A) shows a patterned SAM before incubation with proteins. Because no sufficient contrast could be obtained in topographic mode of the AFM, because of the similar height of both molecules, this image was recorded using the phase mode of the AFM. The phase contrast clearly allows discriminating regions functionalized with the OEG-thiol (squares) from regions functionalized with a mixture of biotin- and OH-thiol (stripes). After incubation with streptavidin the biotinylated parts of the sample can be topographically recognized as bright stripes (Figure 10B₁). A further increase in height is recognized after subsequent incubation with biotinylated peroxidase (Figure 10C₁). In all preparation stages the lateral patterned surface structure fabricated by μ CP can be easily followed. No unspecific adsorption of both proteins to the OEG-terminated regions is observed. In addition, the lateral patterning allows differential height measurements verifying monolayer adsorption of the involved proteins. However, tapping mode AFM has been used because, in earlier studies,¹⁹ we observed that the protein layer is compressed when imaged in contact mode. By using the tapping mode of the AFM, the forces on the proteins are significantly lower and no compression of the protein layer could be detected (Figure 10). Differential height measurements (cross section analyses) of the AFM micrographs are shown in Figure 10A₂ and 10B₂. In the case of streptavidin a step height of (42.2 ± 3) Å is observed, which compares well with the size of streptavidin in its protein crystal structure²⁴ (43–45 Å). After peroxidase adsorption the step height increases to (75.5 ± 4) Å. The difference to the height of streptavidin amounts to (33.3 ± 3) Å and compares well with the height of the shorter side of the peroxidase in its protein crystal structure²⁴ (40–42 Å).

Photometric Activity Tests. In Figure 11 the results of the colorimetric activity test are presented. The upper three spectra represent the activity of the peroxidase in free solution. With increasing incubation times (5, 10, and 15 min) the peak at 452 nm becomes, as expected, more and more pronounced (maximum intensities 0.34, 0.67, and 1.0). These spectra serve as a reference for the maximum enzymatic activity. However, when comparing with the activity obtained for peroxidase immobilized to a streptavidin layer a strong reduction of the 452 nm peaks is observed (lower three spectra, interrupted lines). But still with

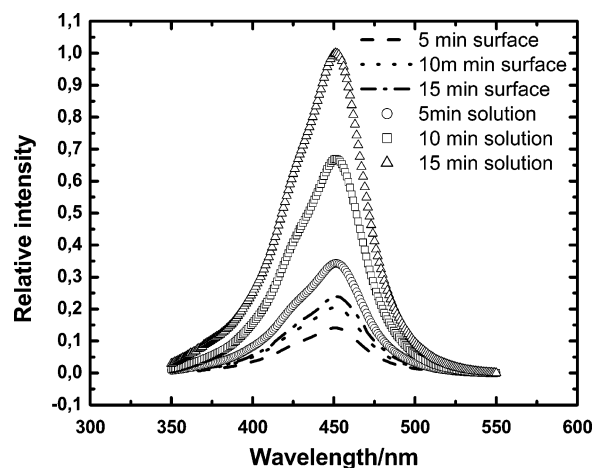


Figure 11. Peroxidase-catalyzed production of a yellow chromogen whose amount is probed by vis spectroscopy after different incubation times. The peak height correlates with the enzyme's activity. In particular, the activity of enzymes in solution is compared with the activity of surface-immobilized enzymes (lower three lines).

increasing incubation time more intense peaks are found (maximum intensities 0.14, 0.20, and 0.24).

When the activity obtained for immobilized peroxidase is compared to that for a streptavidin layer and peroxidase in free solution, the molar ratio of proteins is very precisely the same.²⁵

Discussion

Controlling of Streptavidin Adsorption by Variation of Biotin-Thiol Concentrations. When rationalizing the experiments aimed at controlling the amount of streptavidin adsorption to SAM surfaces by adjusting the biotin-thiol concentration, one has to consider some unpleasant "side effects" associated with this approach. At first glance it seems reasonable to fit a line through the first four data points where the changes in streptavidin adsorption are strongest. The general outcome of the optimization of streptavidin binding to biotin-containing SAMs in dependence of biotin-thiol concentration is in good agreement with previously reported studies²³ where similar profiles have been observed.

The linear fit, indicated in Figure 2, reveals a steep slope of approximately 153 (ng/cm²) per mol % of biotin-thiol and points out that the approach of varying biotin concentrations is impractical for precisely controlling the amount of streptavidin

adsorption. Minor changes in biotin concentration, e.g., arising from evaporation of solvent during incubation cause a large change in the amount of adsorbed streptavidin. One should also note that when working with low numbers of molecules even under careful experimental handling it is difficult to control the amount of molecules that is lost due to unspecific adsorption to walls of incubation vessels, dust particles and impurities. Moreover, a detailed investigation shows that the dependence between streptavidin adsorption and mol % of biotin-thiol is not exactly linear. Even in the interval from 0–1 mol % biotin-thiol the linear fit is a rough estimate, as indicated by a low R^2 value scoring only 0.975. It should also be noted that in previous works it has been pointed out that the molar ratio of thiols solution can noticeably differ from the molar equilibrium ratios within the SAMs.²⁶

Streptavidin Real-Time Adsorption Kinetics. In the adsorption kinetics of streptavidin clearly two phases can be recognized (Figure 4). The first, linear phase is most likely diffusion limited. Close to the surface a streptavidin depletion zone is created because streptavidin binding occurs on a faster time scale than diffusion. Explaining the second phase, which shows a double exponential kinetic behavior (a single exponential behavior did not fit adequate with the experimental data), is more difficult and one has to consider a superimposition of a least two processes with different time constants. Although the involved processes cannot be identified unambiguously from the kinetics alone, in the simplest scenario these two processes would be unspecific adsorption of streptavidin to OH-terminated parts of the SAM in the presence of specific adsorption to biotin head groups. In conclusion, the following naive model can explain the kinetic data: 80% of the applied streptavidin binds with a linear diffusion-limited rate of 0.049 s^{-1} . The two exponential terms obtained by fitting the second, nonlinear phase have almost identical amplitudes (0.54 vs 0.46). However, the kinetic rate constants differ nearly by an order of magnitude (0.081 s^{-1} vs 0.006 s^{-1}). When it is assumed that specific binding occurs faster than unspecific adsorption, the first exponential term could be assigned to specific and the second term to unspecific adsorption. In any case, we have to point out that this is a strong assumption because unfolding events and structural rearrangements that are postulated to govern unspecific adsorption have been reported on fast time scales also.^{27,28} Due to the fact that the amplitude of the exponential terms is nearly equal, our simplified model proposes that further 10% of the streptavidin are adsorbed specifically during the second, nonlinear phase. Nonspecific adsorption is observed for the final 10% of streptavidin molecules. At present we are not able to explain the time constants associated with the different adsorption phenomena. The view derived from the simple model is fully consistent with SPR experiments aimed at checking the amount of unspecific adsorption (Figure 7) as well as the results from the AFM measurements (see below).

Diffusion-Limited Streptavidin Loading. The diffusion-limited loading of streptavidin to a fixed biotinylated matrix has proven to be well suited to adjust reliably the level of desired streptavidin surface density (Figure 5). By carefully choosing concentrations and with some practice, one can control the loading to better than $\pm 5\%$.

Peroxidase Adsorption to Streptavidin. Peroxidase adsorbs under the chosen incubation condition quickly (Figure 6) and selectively (Figures 7 and 8) to the streptavidin anchored on the SAM surface. The slight decrease in the SPR signals found after the incubation with the peroxidase (Figure 6) could arise from different origins which will be discussed in the following.

First, the interaction between peroxidase and streptavidin could be partly transient in its nature and therefore desorption is observed after privation of peroxidase solution. This scenario is unlikely because the equilibrium of the coupling reaction lies strongly on the side of biotin binding with dissociation half-life times in the range of days (see, e.g., ref 2; half-life time ~ 200 days for streptavidin–biotin interaction in solution). Loosely attached material should be removed upon buffer exchange by the fluid stream within seconds but not in a time frame of 30 min.

Second, it has to be mentioned that the peroxidase is tagged between 1.5 and 3 times (on average 2.25 times) with a biotinamidocaproyl group, i.e., the average number of biotin anchors attached to the peroxidase amounts to 2.25. This group can be attached to free amino function only (e.g., Lys side chains) and among these amino functions the attachment is statistically. As a result, a simple one-to-one streptavidin-to-peroxidase interaction cannot be expected. Moreover, multiple biotinylation sites do not only allow for multivalent binding but also for kinetically slow rearrangements of the peroxidase molecules. Upon binding with a first biotin the peroxidase might rearrange its orientation to finally allow another of its biotin to interact with further unoccupied streptavidin molecule. However, rearrangements leading to more compact structures will usually slightly increase the observed SPR signal²⁹ so that this scenario can be ruled out as well.

On the basis of these considerations we propose that the SPR signal decrease is due to a slow desorption of unspecifically adsorbed streptavidin–peroxidase conjugates. As revealed by the previous analysis of the streptavidin adsorption kinetics especially during the high-density loading of streptavidin toward biotinylated SAMs a slight degree of unspecific adsorption is found. After switching back to protein-free running buffer, no changes in the SPR signals are observed (see Figure 5), indicating stable (irreversible) interactions between the SAM-surface and adsorbed proteins. However, when the peroxidase binds to the few unspecifically adsorbed streptavidins this situation can change because upon complex formation the molar mass increases from 66 kDa (streptavidin only) to approximately 110 kDa (streptavidin–peroxidase complex). The previously unspecifically adsorbed streptavidin becomes attached toward a bulky hydrophilic partner, which shifts the equilibrium toward desorption. In this context the observed desorption signal (e.g., ~ 60 RU for the three upper curves in Figure 6) should be compared with the total protein loading of the SAM-surface (2687–3276 RU). With respect to the total protein loading the desorption signals corresponds to a rather small decrease of typically 2.5% only.

This view is also in agreement with the SPR data obtained for the nonspecific adsorption of streptavidin toward an OH-terminated SAM (Figure 7) and the unspecific adsorption of peroxidase toward D-biotin blocked streptavidin monolayers at various streptavidin surface densities (Figure 8).

More interestingly, Figure 9 strongly indicates a density dependent reorientation of the biotinylated peroxidase during binding to streptavidin. At low streptavidin surface densities 1 peroxidase molecule interacts with 2.25 streptavidin molecules, and at high streptavidin densities this ratio changes to an almost one-to-one interaction. Because unspecific adsorption is low (see discussion above and also Figures 7 and 8) the peroxidase must undergo changes in structure or orientation (packing densities) when adsorbing to high streptavidin densities. As will be demonstrated by probing the enzymatic activity (see activity tests below), the peroxidase is still active when immobilized

toward streptavidin, thus a change in orientation upon binding is more likely.

Streptavidin and Peroxidase Adsorption Investigated by AFM. Tapping mode AFM micrographs of the patterned samples show a step height of $42.2 \pm 3 \text{ \AA}$ for streptavidin (see Figure 10). This compares well with the height of SA of $43\text{--}45 \text{ \AA}$ as derived from the bulk structure.²⁴ For the protein bilayer (streptavidin plus peroxidase) a step height of $75.5 \pm 4 \text{ \AA}$ was detected (see Figure 10), yielding a step height for bHRP of $33.3 \pm 3 \text{ \AA}$ in good agreement with the height of shorter side of bHRP ($40\text{--}42 \text{ \AA}$) from bulk structure.²⁴ On the basis of the high spatial resolution of the AFM measurements, we can conclude that there are no or very few defects in the adsorbed protein layers (see Figure 10). The adsorption of SA leads to a monolayer where the protein retains its biological activity (binding of biotin). This is shown by the binding of bHRP, which also leads to a complete monolayer. As expected, there is no adsorption of the proteins observed on the stamped protein repellent OEG-thiol areas. Generally, the AFM results are fully consistent with the SPR data above. However, we did not succeed in recognizing single streptavidin molecules on the biotinylated stripes, which is necessary for a real molecular understanding of the open SPR issues, e.g., measuring streptavidin surface densities by counting single molecules, discriminating specific vs nonspecific adsorbed proteins, or answering the question of structural rearrangements during peroxidase adsorption.

Photometric Activity Tests. During the enzymatic activity test the colorless chromogen 3,3',5,5'-tetramethylbenzidine (TMB) is converted into a blue product (TMB charge-transfer complex) which by addition of an acid is converted into a stable yellow dye with maximum absorbance around 450 nm.

In “negative control” experiments the absorbance in the spectral range from 350 to 550 nm was checked after omission of the peroxidase protein during incubation. As expected, these experiments revealed a flat baseline without absorbance around 450 nm (data not shown).

In “positive control” experiments peroxidase was dissolved into buffer. Then the enzymatic activity was measured with dependence on substrate incubation time (Figure 11). The maximum intensity values of these spectra are found at 452 nm and can be fitted to a linear function passing through the origin (absorbance at $\lambda_{\text{max}} = 0.0669 \times \text{incubation time}/\text{min}$; $R^2 = 0.9998$).

In comparison to the high enzymatic activity found for the free peroxidase in buffer, the enzymatic activity of peroxidase after binding toward surface-immobilized streptavidin is apparently significantly reduced (Figure 11). The maximum intensity is also found at 452 nm, but in contrast to the solution experiments, the maximum intensity cannot be fitted to a linear function passing through the origin (absorbance at $\lambda_{\text{max}} = 0.01 \times \text{incubation time}/\text{min} + 0.0933$; $R^2 = 0.9868$). These findings can be rationalized by considering that in solution all sides of the peroxidase can be easily reached by the substrate molecules; on the surface at high densities only the upper side is directly accessible. The lateral sides and the backside are efficiently blocked by other peroxidase molecules or the streptavidin supporting layer. Therefore a naïve comparison of the maximum intensities obtained from the spectra overestimates the apparent reduction in enzymatic activity: e.g., after 15 min of incubation a 4-fold reduction in activity would be concluded from maximum intensities 1 (solution) vs 0.24 (surface).

According to Michaelis–Menten enzyme kinetics a maximum enzymatic turn over is found when enzymes (E) are completely

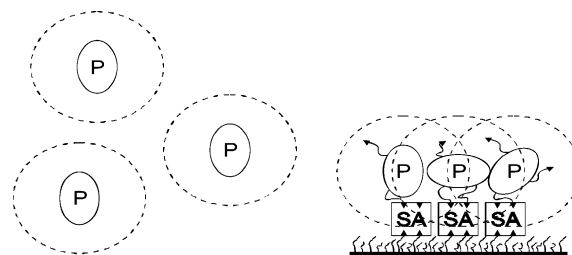


Figure 12. “Diffusion spheres” of each peroxidase (P) enzyme. All substrate molecules that are in that sphere can reach the active site of the enzyme in a given time. On the left, the situation in solution is depicted where plenty of space is available between the enzymes so that no overlapping of diffusion spheres is observed. On the right, the situation for surface-immobilized enzymes is drawn. Now the peroxidase molecules are concentrated in a protein monolayer in close proximity of the streptavidin (SA) surface. Consequently, the diffusion spheres are overlapping and the peroxidase enzymes are competing for substrate molecules. Please note the asymmetric shape of peroxidase and its multivalency in biotin anchors, which allows for multiple orientations at the surface.

saturated with substrate (S) molecules ($[S] \gg [E]$). This condition is fulfilled in experiments probing peroxidase activity in solution because at the molecular scale the enzymes are well separated from each other with an imaginary nonoverlapping diffusion sphere around each enzyme (see Figure 12). Only the substrate molecules inside the diffusion sphere can be turned into product during the time course of the experiment. The linear fit function of the maximum intensities of the 452 nm peaks passing through the origin is verifying this molecular image by indicating a constant turnover speed throughout the solution activity experiment. When peroxidase is bound to the surface, the situation is completely different. All peroxidase molecules are now immobile and located in close proximity to each other. The imaginary diffusion spheres are strongly overlapping and also blocked by the solid support (glass support, SAM surface, and streptavidin layer; see Figure 12). Therefore the enzymes are strongly competing for substrate molecules and soon after a short time of high enzymatic activity (e.g., immediately after dipping the peroxidase covered surfaces into the substrate solution) the substrate molecules close to the surface will be depleted. Due to the lack of substrate molecules the turnover rate of peroxidase enzymes will be reduced. This is also the reason why the linear fit function of the maximum intensities of the 452 nm peaks in the surface activity experiment is not passing through the origin.

A quantitative view will need a more precise treatment of the diffusion processes in solution and close to the surface. Nevertheless, the colorimetric activity tests clearly demonstrate that the peroxidase retains its biological activity after binding toward surface-immobilized streptavidins.

Conclusions

We have investigated the anchoring of a biotinylated peroxidase on a two-dimensional patterned array of streptavidin, which was assembled in a two-step process. First, a two-dimensionally patterned biotinylated SAM surface was generated using μ -contact printing onto which a streptavidin layer was bound specifically. By employing a number of different techniques (SPR, AFM, and absorption spectroscopy), one can obtain a rather detailed and consistent picture of the peroxidase adsorption processes.

The presence of a highly specific interaction of the peroxidase with streptavidin could be shown by monitoring the adsorption of peroxidase for different streptavidin surface densities. There

is indirect evidence that the orientation of the peroxidase depends on the streptavidin coverage: At low streptavidin densities a molecular ratio between peroxidase and streptavidin of 1:2.25 was found, which changed to a ratio of 1:1 at higher streptavidin coverage.

Imaging patterned SAMs with AFM revealed the specific adsorption of a homogeneous protein monolayer. The biological activity of the peroxidase enzyme was probed by absorption spectroscopy using a test reaction involving a chromophore and revealed that the surface-anchored peroxidase is still active. For the surface-immobilized enzymes a reduction in enzymatic activity to 30–40% of the solution activity is appointed on the basis of the decrease in the measured absorption maxima. However, this view still ignores the overlapping of the enzyme's "diffusion spheres" when bound to the surface; therefore the actual peroxidase activity will be higher. In future studies it will be interesting to investigate the influence of the orientation of the peroxidase. To this end we plan to use peroxidase molecules with site-specific attachment of biotin. The surface activity can then be tuned by controlling the attachment site, which provides a better starting point for quantitative activity measurements of immobilized enzymes.

Acknowledgment. C.G. thanks the Alexander-von-Humboldt foundation for a Feodor-Lynen postdoctoral fellowship.

References and Notes

- (1) Knoll, W.; Zizlsperfer, M.; Liebermann, T.; Arnold, S.; Liley, M.; Ciscevic, D.; Schmitt, F. J.; Spinke, J. *Colloids Surf. A* **2000**, *161*, 115–137.
- (2) Wilchek, M.; Bayer, E. A. *Avidin-Biotin Technol.* 1990; Vol. 184.
- (3) Liu, J. Y.; Tiefenauer, L.; Tian, S. J.; Nielsen, P. E.; Knoll, W. *Anal. Chem.* **2006**, *78* (2), 470–476.
- (4) Su, X. D.; Wu, Y. J.; Robelek, R.; Knoll, W. *Langmuir* **2005**, *21* (1), 348–353.
- (5) Niemeyer, C. M.; Sano, T.; Smith, C. L.; Cantor, C. R. *Nucleic Acids Res.* **1994**, *22* (25), 5530–5539.
- (6) Niemeyer, C. M.; Boldt, L.; Ceyhan, B.; Blohm, D. *Anal. Biochem.* **1999**, *268* (1), 54–63.
- (7) Huber, C.; Liu, J.; Egelseer, E. M.; Moll, D.; Knoll, W.; Sleytr, U. B.; Sara, M. *Small* **2006**, *2* (1), 142–150.
- (8) Ladd, J.; Boozer, C.; Yu, Q. M.; Chen, S. F.; Homola, J.; Jiang, S. *Langmuir* **2004**, *20* (19), 8090–8095.
- (9) Niemeyer, C. M. *Nantoday* **2007**, *2* (2), 42–52.
- (10) Schmidt, H.-L.; Schumann, S. W.; Scheller, F. VCH: Weinheim, 1992; Vol. 3, Chapter 14.5.1, pp 761–764.
- (11) Willner, I.; Katz, E. VCH: Weinheim, 1999; Vol. 5, Chapter 2, p 63.
- (12) Willner, I. VCH: Weinheim, 2005; Chapter 3.
- (13) Gottenbos, B.; Busscher, H. J.; van der Mei, H. C. *J. Mater. Sci.—Mater. Med.* **2002**, *13* (8), 717–722.
- (14) Stickler, D. J.; McLean, R. J. C. *Cells Mater.* **1995**, *5* (2), 167–182.
- (15) Chen, C. S.; Mrksich, M.; Huang, S.; Whitesides, G. M.; Ingber, D. E. *Science* **1997**, *276* (5317), 1425–1428.
- (16) Ostuni, E.; Yan, L.; Whitesides, G. M. *Colloids Surf. B: Biointerfaces* **1999**, *15*, 3–30.
- (17) Gettens, R. T. T.; Bai, Z. J.; Gilbert, J. L. *J. Biomed. Mater. Res. Part A* **2005**, *72A* (3), 246–257.
- (18) Ying, P. Q.; Yu, Y.; Jin, G.; Tao, Z. L. *Colloids Surf. B: Biointerfaces* **2003**, *32* (1), 1–10.
- (19) Grunwald, C.; Eck, W.; Opitz, N.; Kuhlmann, J.; Wolf, C. *Phys. Chem. Chem. Phys.* **2004**, *6* (17), 4358–4362.
- (20) Josephy, P. D.; T. E.; Mason, R. P. *J. Biol. Chem.* **1982**, *257* (7), 3669–3675.
- (21) Ostuni, E.; Chapman, R. G.; Liang, M. N.; Meluleni, G.; Pier, G.; Ingber, D. E.; Whitesides, G. *Langmuir* **2001**, *17* (20), 6336–6343.
- (22) Kumar, A.; Biebuyck, H. A.; Whitesides, G. M. *Langmuir* **1994**, *10* (5), 1498–1511.
- (23) Spinke, J.; Liley, M.; Schmitt, F. J.; Guder, H. J.; Angermaier, L.; Knoll, W. *J. Chem. Phys.* **1993**, *99* (9), 7012–7019.
- (24) Bank, R. P. D. www.rcbs.org, 2005.
- (25) The amount of enzyme was calculated as follows: First the amount of adsorbed mass per cm² was calculated from the SPR measurement. From this we calculated the mass for the complete area of the wafers used for the activity test. Then we determined how many microliters of our standard 150 nM peroxidase solution fits this. This volume (in the region of 3–5 μ L) was added to 1 mL of the substrate buffer (standard volume for the activity test).
- (26) Nelson, K. E. *Langmuir* **2001**, *17* (9), 2807–2816.
- (27) Czeslik, C. Z. *Phys. Chem.—Int. J. Res. Phys. Chem. Chem. Phys.* **2004**, *218* (7), 771–801.
- (28) Herrwerth, S.; Eck, W.; Reinhardt, S.; Grunze, M. *J. Am. Chem. Soc.* **2003**, *125* (31), 9359–9366.
- (29) Zako, T.; Harada, K.; Mannen, T.; Yamaguchi, S.; Kitayama, A.; Ueda, H.; Nagamune, T. *J. Biochem.* **2001**, *129*, 1–4.